

# Local SVD based NIR Face Retrieval

Shiv Ram Dubey\*<sup>1</sup>, Satish Kumar Singh<sup>2</sup>, Rajat Kumar Singh<sup>2</sup>

<sup>1</sup>Indian Institute of Information Technology Chittoor, Sri City, India

<sup>2</sup>Indian Institute of Information Technology Allahabad, India

\*Corresponding Author: Email: shivram1987@gmail.com

This paper is accepted and published by *Journal of Visual Communication and Image Representation, Elsevier*.

DOI: <https://doi.org/10.1016/j.jvcir.2017.09.004>

The copyright is transferred to Elsevier.

Cite this paper as: S.R. Dubey, S.K. Singh, and R.K. Singh, Local SVD based NIR Face Retrieval. *Journal of Visual Communication and Image Representation*, 2017 (DOI: <https://doi.org/10.1016/j.jvcir.2017.09.004>).

**Abstract**— From last decade, local descriptor such as Local Binary Pattern (LBP) is accepted as a very prominent feature descriptor for characterizing the images such as faces. The performance of such descriptors depends upon the local relationship of the image. The local relationship of the image can be utilized in more discriminative and robust way after some preprocessing as compared to the original image. The preprocessed images in the form of 4 sub-bands (i.e. S, U, V, and D sub-bands) are obtained by applying the Singular Value Decomposition (SVD) over the original image. The local descriptors are computed over these sub-bands (mainly S sub-band) and termed as the SVD based local descriptors. The performance of four local descriptors over SVD sub-bands are tested for near-infrared face retrieval using PolyU-NIR and CASIA-NIR face databases, and compared with the results obtained using descriptors without SVD sub-band. The experimental results confirm the superiority of using S sub-band of SVD in terms of performance of the local descriptors over NIR face databases.

**Index Terms**—Local features, near-infrared face image, face retrieval, singular value decomposition, local binary pattern.

## I. INTRODUCTION

The efficient content based image retrieval (CBIR) is still an evolving research area in the field of Computer Vision and Image Processing [1]. Any CBIR system retrieves the most similar images of a given query image from the huge databases. The CBIR approaches mainly retrieve the similar images on the basis of the information contained in the image [2].

Face retrieval can be seen as a special case of image retrieval where faces of the same person are retrieved against a query face. Park and Jain have proposed to use the demographic information (e.g., gender and ethnicity) and facial marks (e.g., scars, moles, and freckles) for facial analysis and retrieval [3]. Very recently, a face recognition survey argued that the improvement in radical face representations/descriptors is the next step in the advancement of facial analytical approaches [4]. Some recent face recognition methods are depicted in [5]-[7]. Face retrieval can be seen as a special case of image retrieval where faces of the same person are retrieved against a query face. In this paper, face retrieval is performed instead of face recognition because in recognition only one top matching image is obtained, whereas in retrieval multiple top matching images are retrieved in decreasing order of similarity.

The performance of any retrieval system is greatly governed by the efficient description of the image features such as color, texture, shape, structure, etc. [12]-[14]. An illumination compensation mechanism is proposed in [12] for those conditions where illumination robust image matching is required. This illumination compensation is restricted to the color images only, whereas NIR images are mostly gray-scaled images. Various image feature descriptors have been introduced by several researchers amongst which the Local Binary Pattern (LBP) is most frequently used [15]. Completed Local Binary Pattern [16], Interleaved Intensity Order Based Local Descriptor [17], Data Driven Local Binary Pattern [18], Local Diagonal Extrema Pattern [19], Local Bit-Plane Decoded Pattern [20] and Local Binary Pattern Histogram Fourier [21], Local Wavelet Pattern [50], Multichannel Decoded Local Binary Pattern [51] etc. are the descriptors proposed as the variants of LBP for textural and medical image analysis. The LBP has shown very promising results for facial analysis also [22]-[23]. Some recent state-of-the-art variants of LBP proposed for the face recognition are Semi-structure Local Binary Patterns [24], Directional Binary Code [8] and Local Gabor Binary Pattern [25], Local Derivative Pattern [26], extended Local Binary Patterns [27], Local Patterns of Gradients [28], Patterns of Gradient Orientations and Magnitudes [29], and Monogenic Binary Coding [30].

There may be situations where visible lights are not available. In such conditions, the Near-infrared (NIR) cameras are capable to capture the images. Thus, it is required to investigate the approaches for image analysis for NIR images. Moreover, the NIR imaging is more useful for the indoor and cooperative-users. The NIR facial analysis is an open challenge in current days [8]-[9]. The images of the same face under different lighting directions in NIR imaging are highly correlated, whereas it is negatively correlated under visible light [9]. The performance of human as well as machine under near-infrared light and visible light is investigated by Hollingsworth *et al.* using periocular biometrics [10]. In a recent study of visual versus near-infrared face image matching [11], the authors have used an NIR face image as the probe while enrollment is done with the visual face images. Due to the importance of NIR face images under indoor/office environments, the NIR face retrieval approach is presented in this paper.

The Singular Value Decomposition (SVD) is one of the most elemental matrix computations in numerical linear algebra [31]. It can be simply termed as the extended version of the theory of linear filtering or a tool for the image enhancement [32]-[33]. SVD has several uses such as in signal analysis [34], gate characterization [35], image coding [36], image watermarking [37], image steganalysis [38], image compression [39], and face recognition [40], etc. A novel concept of sub-band decomposition and multi-resolution representation of digital color images using SVD is introduced by Singh *et al.* [41]. They have basically applied the SVD over regions of the image and finally formed 4 sub-bands. In this paper, we also used the same approach as used in [41] for SVD based sub-band computation of the near-infrared (NIR) face images. The SVD over the whole face image is used for the illumination robust face recognition in [42]-[43]. Inspired from the success of SVD over whole face image [40], [42]-[43], we formed SVD sub-bands [41] over face regions to overcome the bad lighting problem of NIR face images. Some researchers use other decomposition techniques, such as semi-discrete decomposition (SSD) [52], to find out the original single image and its transpose in the training set for computing the intra-class scatter matrices; the intra-class maximum–minimum–median average vector is used in maximum scatter difference (MSD) model for face recognition [53]; intra-class scatter matrix null space median method, QR factorization, QR decomposition weighted kernel discriminant analysis and Kernel Fuzzy Discriminant Analysis are used for face recognition task [54-57]. The main difference between proposed method and [52-57] is that the proposed method utilizes the local factorization and local relationship to form the descriptor, whereas, the global factorization is performed in [52-57]; the proposed descriptor does not depend upon the training data, whereas, [52-57] depend upon the training data.

SVD basically represents local information contained in an image, in a more robust way [31], whereas local descriptors such as Local Binary Pattern (LBP) [15], Semi-structure Local Binary Pattern (SLBP) [24], Directional Binary Code (DBC) [8] and Local Gabor Binary Pattern (LGBP) [25] encode the local information of the image in the descriptor form. Basically, the image descriptors computed over the raw intensity values missed to utilize the local spatial relationship because they encode the occurrences of the pattern over the image. If they divide the image into sub-regions, then the dimension of descriptor become too high to be fit for the image matching due to time constraint. These are the driving factors for us to combine the SVD with local feature descriptors to propose the new SVD based local feature descriptors in this paper. We encode the descriptors over SVD sub-band images instead of the original image. The SVD sub-band formation actually exploits the local spatial information by encoding the relationship of each  $2 \times 2$  non-overlapping sub-regions of the image. This behavior is very useful to explore the local relationship of Near-Infrared images where the images are captured mostly in very bad lighting conditions and computing descriptors directly over it are not able to capture the local information accurately. We have performed the face retrieval experiments over two NIR face database, namely PolyU-NIR [44] and CASIA-NIR [45]. From the experiments, very promising results are found and observed that the performance of local descriptors is improved when it is constructed over the S sub-band of the SVD decomposition. The followings are the key contributions:

1. We have explored the possibility to utilize the Local SVD for image representation.
2. We have explored the commentary nature of Local SVD and Local descriptors.
3. We have performed the SVD and Local descriptor based image retrieval over NIR face databases.
4. We have also tested the suitability of different distance measures in the proposed context.

The continuing sections of this paper are the description of the proposed NIR face retrieval system in section 2, performance measure and evaluation criteria in section 3, NIR face image retrieval experiments, results and observations in section 4 and conclusion in section 5.

## II. PROPOSED SVD SUB-BAND BASED NIR FACE RETRIEVAL

The proposed framework for NIR face retrieval is illustrated in Fig. 1. It consists of four main components, namely Singular Value Decomposition (SVD) sub-band formation, local descriptor extraction, feature vector

computation and similarity measurement and NIR face retrieval. The feature vector is formed using the extracted local descriptors over the SVD sub-bands obtained by applying SVD decomposition over each face image of the database as well as query face image. The face retrieval is performed by finding the best similarities between the feature vector of query face with the feature vectors of the database faces. In this section, we will describe each component of the introduced methodology in details.

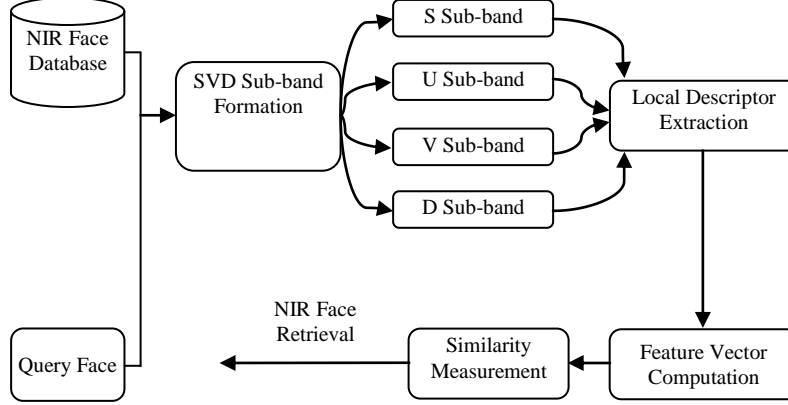


Fig. 1. The proposed framework for NIR face retrieval using SVD Sub-bands. All the face images including query also are decomposed in four sub-bands using SVD block based decomposition. The S sub-band basically contains the low frequency information, whereas the remaining sub-bands contain the high frequency information. The local descriptors are computed over the SVD sub-band images and used to find out the best matching faces against the query face.

#### A. SVD Sub-bands Formation

This sub-section is devoted to a description of the construction process of the sub-bands of the singular value decomposition (SVD) at a particular level (i.e. multi-resolution) over a given image. The SVD based sub-band decomposition and multi-resolution representation [41] are used to enhance the features of the original image (i.e. to cope with the illumination problem of the NIR imaging).

Let  $I^{i,j}$  is the intensity value of any pixel at  $i^{th}$  row and  $j^{th}$  column of any gray scaled NIR face image  $M$  having  $m_x$  rows and  $m_y$  columns (i.e. the total number of pixels in  $M$  is  $m_x \times m_y$ ). Let  $P_L$  is the input image of dimension  $m_x^L \times m_y^L$  for the  $L^{th}$  level of SVD factorization. The input image  $P_L$  is first divided into  $2 \times 2$  non-overlapping blocks, then SVD is applied over each block. Thus, a total  $n^L = n_x^L \times n_y^L$  number of SVD is required, where  $n_x^L = \lfloor m_x^L / 2 \rfloor$  and  $n_y^L = \lfloor m_y^L / 2 \rfloor$ . Let  $P_{L,t_x,t_y}$  represents the  $(t_x, t_y)^{th}$  block of image  $P_L$ . By above convention,  $P_L^{i,j}$  represents the intensity value of the pixel at  $i^{th}$  row and  $j^{th}$  column of image  $P_L$ . The intensity values of the  $(t_x, t_y)^{th}$  block of the image  $P_L$  are given as follows,

$$P_{L,t_x,t_y} = \begin{bmatrix} P_L^{2t_x-1,2t_y-1} & P_L^{2t_x-1,2t_y} \\ P_L^{2t_x,2t_y-1} & P_L^{2t_x,2t_y} \end{bmatrix} \quad (1)$$

where  $t_x \in [1, n_x^L]$  and  $t_y \in [1, n_y^L]$ .

The SVD of  $(t_x, t_y)^{th}$  block of  $P_L$  (i.e.  $P_{L,t_x,t_y}$ ) can be represented in the following factorization form,

$$P_{L,t_x,t_y} = (A_{L,t_x,t_y})(B_{L,t_x,t_y})(C_{L,t_x,t_y})^T \quad (2)$$

where  $A_{L,t_x,t_y}$  and  $C_{L,t_x,t_y}$  are  $2 \times 2$  matrices containing the orthogonal column vectors, and  $B_{L,t_x,t_y}$  is a  $2 \times 2$  diagonal matrix having singular values at the main diagonals.

We can write Eq. (2) as follows,

$$\begin{bmatrix} P_L^{2t_x-1,2t_y-1} & P_L^{2t_x-1,2t_y} \\ P_L^{2t_x,2t_y-1} & P_L^{2t_x,2t_y} \end{bmatrix} = \begin{bmatrix} A_L^{2t_x-1,2t_y-1} & A_L^{2t_x-1,2t_y} \\ A_L^{2t_x,2t_y-1} & A_L^{2t_x,2t_y} \end{bmatrix} \begin{bmatrix} B_L^{2t_x-1,2t_y-1} & B_L^{2t_x-1,2t_y} \\ B_L^{2t_x,2t_y-1} & B_L^{2t_x,2t_y} \end{bmatrix} \begin{bmatrix} C_L^{2t_x-1,2t_y-1} & C_L^{2t_x-1,2t_y} \\ C_L^{2t_x,2t_y-1} & C_L^{2t_x,2t_y} \end{bmatrix}^T \quad (3)$$

where  $B_L^{2t_x-1,2t_y} = B_L^{2t_x,2t_y-1} = 0$ .

The four sub-bands at  $L^{th}$  level, namely  $S_L$ ,  $U_L$ ,  $V_L$  and  $D_L$  are formed from Eq. (3) as follows,

$$S_L^{t_x,t_y} = B_L^{2t_x-1,2t_y-1} \quad (4)$$

$$U_L^{t_x,t_y} = A_L^{2t_x-1,2t_y-1} \quad (5)$$

$$V_L^{t_x,t_y} = C_L^{2t_x-1,2t_y-1} \quad (6)$$

$$D_L^{t_x,t_y} = B_L^{2t_x,2t_y} \quad (7)$$

The input image  $P_L$  for SVD at  $L^{th}$  level is defined recursively in terms of the original image ( $I$ ) and S sub-band ( $S_{L-1}^{t_x,t_y}$ ) at  $(L-1)^{th}$  level as follows:

$$P_L = \begin{cases} I & \text{if } L = 1 \\ S_{L-1}^{t_x,t_y} & \text{Otherwise} \end{cases} \quad (8)$$

Similarly, the dimensions of  $P_L$  (i.e.  $m_x^L$  and  $m_y^L$ ) are also defined recursively as follows,

$$m_x^L = \begin{cases} m_x & \text{if } L = 1 \\ \left\lfloor \frac{m_x^{L-1}}{2} \right\rfloor & \text{Otherwise} \end{cases} \quad (9)$$

$$m_y^L = \begin{cases} m_y & \text{if } L = 1 \\ \left\lfloor \frac{m_y^{L-1}}{2} \right\rfloor & \text{Otherwise} \end{cases} \quad (10)$$

In order to find the multi-resolution sub-bands, the S sub-band obtained in the previous level is treated as the input image. An example of SVD based sub-band formation is illustrated in Fig. 2. Four sub-bands, namely S, U, V and D of size  $2 \times 2$  each are created from the input of size  $4 \times 4$ . In Fig. 3(a), the sub-bands for an input image are displayed up to the 2<sup>nd</sup> level of SVD decomposition. Note that, the sub-bands are shown in the order of  $S_2$ ,  $U_2$ ,  $V_2$ ,  $D_2$ ,  $U_1$ ,  $V_1$  and  $D_1$ . The original image and the approximation sub-bands (i.e. S sub-band) at 1<sup>st</sup> and 2<sup>nd</sup> level of the SVD factorization are visualized in the form of a pyramid in the Fig. 3(b) with S sub-band of 2<sup>nd</sup> level at the top of the pyramid.

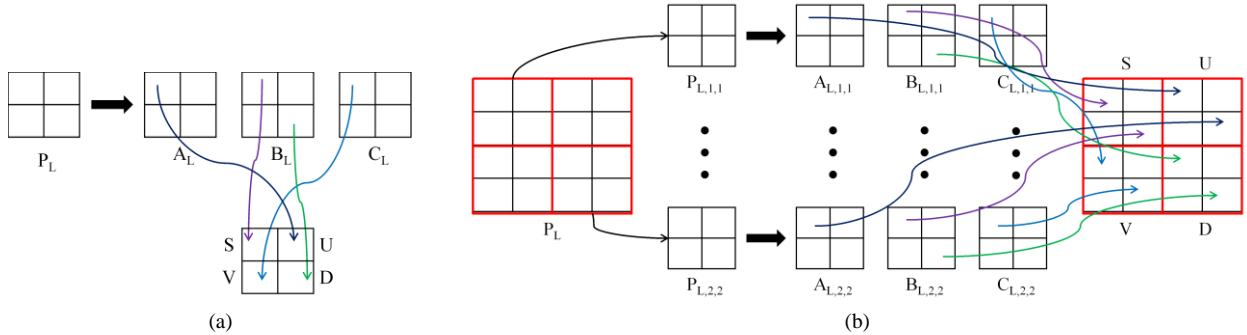


Fig. 2. (a) Illustration of the sub-band formed (i.e. S, U, V and D sub-bands) from the SVD factorization of any input  $P_L$  using an example of size  $2 \times 2$ , and (b) Illustration of the sub-band formed (i.e. S, U, V and D sub-bands) from the SVD factorization of any input  $P_L$  using an example of size  $4 \times 4$ . The S sub-band consist the information related to the largest local eigenvalues.

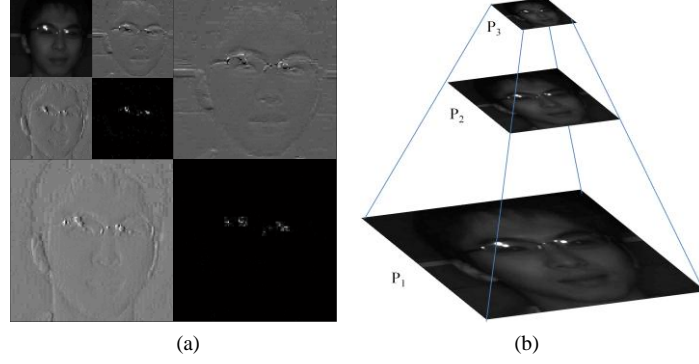


Fig. 3. (a) An example of SVD decomposition at 2<sup>nd</sup> level, and (b) Original image is superimposed by the S sub-bands at 1<sup>st</sup> and 2<sup>nd</sup> level. The image is taken from the PolyU-NIR Face database. The low frequency information (i.e. ambience) in S sub-band and the high frequency information (i.e. horizontal, vertical and diagonal details) in U, V, and D sub-bands can be easily observed. At each level of decomposition, the resolution of the image is getting half similar to a pyramid.

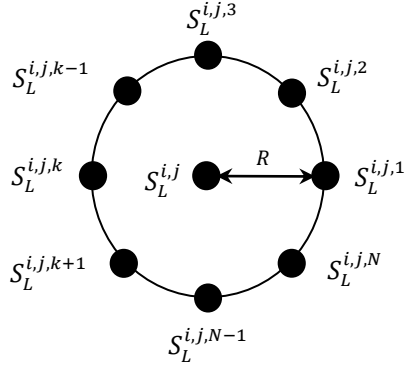


Fig. 4. The coordinates of the  $N$  local neighbors of a center pixel  $(i, j)$ . Here,  $S_L^{i,j}$  represents a pixel at coordinate  $(i, j)$  in S sub-band image at  $L^{\text{th}}$  level. The  $S_L^{i,j,k}$  is the  $k^{\text{th}}$  neighbor of  $S_L^{i,j}$  in a circular fashion.

### B. Local Descriptor Extraction

In this sub-section, we introduce to extract the local descriptors over the sub-band face images obtained after applying the SVD at a particular level over the original face image. In order to show the significance of local descriptor construction over SVD sub-bands for NIR face retrieval, we extracted Local Binary Pattern (LBP) [15], Semi-structure Local Binary Pattern (SLBP) [24], Directional Binary Code (DBC) [8] and Local Gabor Binary Pattern (LGBP) [25] based local descriptors.

The LBP descriptors computed over S, U, V, and D sub-bands are denoted as the SVD-S-LBP, SVD-U-LBP, SVD-V-LBP and SVD-D-LBP respectively. The LBP operator is applied over the S sub-band of SVD at  $L^{\text{th}}$  level (i.e.,  $S_L$  sub-band) to form the descriptor. The SVD-S-LBP value for  $S_L^{i,j}$  is computed as follows,

$$SVD - S - LBP_L^{i,j} = \sum_{k=1}^N (2)^{k-1} \times f_1(S_L^{i,j,k}, S_L^{i,j}) \quad (11)$$

where  $S_L^{i,j}$  represents the center pixel at coordinates  $(i, j)$  of  $S_L$  sub-band,  $S_L^{i,j,k}$  represents the  $k^{\text{th}}$  neighbor of pixel  $S_L^{i,j}$  in  $S_L$  sub-band when  $N$  neighbors evenly distributed at a radius  $R$  centered at  $(i, j)$  are considered for the LBP computation (see Fig. 4), and  $f_1(\alpha, \beta)$  is defined as follows,

$$f_1(\alpha, \beta) = \begin{cases} 1 & \text{if } \alpha \geq \beta \\ 0 & \text{Otherwise} \end{cases} \quad (12)$$

Similarly, the LBPs over the remaining sub-bands of SVD at a  $L^{\text{th}}$  level (i.e.,  $U_L$ ,  $V_L$ , and  $D_L$  sub-bands) are computed as follows,

$$SVD - U - LBP_L^{i,j} = \sum_{k=1}^N (2)^{k-1} \times f_1(U_L^{i,j,k}, U_L^{i,j}) \quad (13)$$

$$SVD - V - LBP_L^{i,j} = \sum_{k=1}^N (2)^{k-1} \times f_1(V_L^{i,j,k}, V_L^{i,j}) \quad (14)$$

$$SVD - D - LBP_L^{i,j} = \sum_{k=1}^N (2)^{k-1} \times f_1(D_L^{i,j,k}, D_L^{i,j}) \quad (15)$$

The other local descriptors (i.e. SLBP, DBC and LGBP) are also computed over each sub-bands of SVD at  $L^{\text{th}}$  level. The naming convention for SLBP, DBC and LGBP over  $S_L$ ,  $U_L$ ,  $V_L$ , and  $D_L$  sub-bands are similar to LBP over these sub-bands.

### C. Feature Vector Computation

In order to represent the feature vector for the patterns  $ptn$  (i.e. SVD-S-LBP, SVD-U-LBP, SVD-V-LBP and SVD-D-LBP), the histograms are computed as follows,

$$\mathcal{H}(\gamma) = \sum_{i=R+1}^{\lfloor \frac{m_x^L}{2} \rfloor - R} \sum_{j=R+1}^{\lfloor \frac{m_y^L}{2} \rfloor - R} f_2(ptn_L^{i,j}, \gamma) \quad (16)$$

for  $\gamma = (0, 2^N - 1)$ , where  $f_2(\alpha, \beta)$  is defined as,

$$f_2(\alpha, \beta) = \begin{cases} 1 & \text{if } \alpha = \beta \\ 0 & \text{Otherwise} \end{cases} \quad (17)$$

and,  $ptn_L^{i,j}$  is the decimal value of patterns at coordinates  $(i, j)$  and computed in (11), (13), (14) and (15) for SVD-S-LBP, SVD-U-LBP, SVD-V-LBP and SVD-D-LBP respectively.

Similarly, we also computed the SLBP, DBC and LGBP feature vectors over each sub-band of the SVD. The dimension of local descriptors doesn't depend upon the SVD (i.e. the dimension of descriptors in conjunction with the SVD sub-band is same as without SVD).

## III. PERFORMANCE MEASURE & EVALUATION CRITERIA

In this section, we describe the several similarity measures as well as evaluation criteria to depict the improved performance of proposed face retrieval using SVD sub-bands and local descriptors over NIR face databases.

### A. Similarity Measures

The main aim of similarity measure is to compute the distance between the feature vectors of two images. Different similarity measures such as Euclidean, Cosine, Emd, Canberra, L1, D1 and Chi-square ( $\chi^2$ ) [46]-[47] are used in this paper to find out the dissimilarity score between the descriptors of the two face images.

### B. Evaluation criteria

We have presented the results using average retrieval precision (ARP), average retrieval rate (ARR), F-measure (F), and average normalized modified retrieval rank (ANMRR) as the functions of the number of top matches or number of retrieved images ( $\eta$ ) [13] [14] [48].

ARP (%) and ARR (%) are computed by taking the means of the average precision and average recall respectively over each category of the database. Average precision and average recall for a category is calculated by

taking the means of the precision and recall respectively, over each image of that category (i.e. each image is used as the query image). For any query image ( $Q$ ), the precision and recall are computed as follows,

$$Precision = \frac{\bar{r}(Q)}{\eta} \quad (18)$$

$$Recall = \frac{\bar{r}(Q)}{\bar{g}(Q)} \quad (19)$$

where  $\bar{r}$  and  $\bar{g}$  are the number of relevant retrieved images and the number of relevant ground truth images for any query image. For computing the F-measure (F) in percentage, we have retrieved the  $max(\eta)$  number of images, where  $max(\eta)$  is the maximum number of images in any category of the database.

$$F = \frac{2 \times ARP \times ARR}{ARP + ARR} \quad (20)$$

We have followed the steps provided in [48] to calculate the ANMRR metric and represented in the percentage in the results of this paper. The lower value of ANMRR represents the better retrieval performance and vice-versa, whereas the higher value of ARP, ARR and F means the better retrieval performance and vice-versa.

#### IV. EXPERIMENTS AND RESULTS

The introduced SVD based local descriptors are used in the near-infrared (NIR) face image retrieval experiments to investigate its performance and discriminating ability. The number of local neighbors  $N$  and radius of neighborhood  $R$  are set to 8 and 1 respectively, in all the experiments of this paper to compute all the descriptors. The state-of-the-art descriptors such as LBP ( $dim: 256$ ) [15], SLBP ( $dim: 256$ ) [24], DBC ( $dim: 8 \times 256$ ) [8] and LGBP ( $dim: 9 \times 256$ ) [25] are used for the comparison of results with and without SVD. We compared the results of SVD based descriptor with the results of original descriptor (i.e. without SVD). For example, the results of SVD-S-LBP are compared with the results of LBP, and so on for other descriptors also. We have used the online available code [49] of LBP, whereas we implemented SLBP, DBC and LGBP following its algorithms. In the computation of DBC, gradients at 0, 45, 90 and 135 degrees are considered. For computation of LGBP descriptor, we have considered three scales and three orientations of Gabor filtering. When not stated, SVD sub-bands at level 1 are used to create the descriptors. Two benchmark NIR face databases, namely PolyU-NIR [44] and CASIA-NIR [45] is used for the face retrieval experiments. We have considered the set-1 of the PolyU-NIR face database which consists of the total 7277 images from 55 subjects with varying number of images per subject. CASIA-NIR face database is comprised of the total 3940 images from the 197 subjects having 20 faces each. The face region of the CASIA-NIR face database is cropped because too much variation is present in the background of the images in this database. The databases are having variations like pose, expressions, scale, etc.

##### A. Experiments over Different Similarity Measures

We have compared the retrieval performance of SVD-S-LBP using different Euclidean, Cosine, Emd, Canberra, L1, D1 and  $\chi^2$  distance measures and reported the results in terms of the ARP, ARR, F and ANMRR in the Table 1 and Table 2 over PolyU-NIR, CASIA-NIR face databases respectively. The ARP, ARR and F are highest, while ANMRR is lowest when the  $\chi^2$  distance is used as the similarity measure for both databases. In the rest of the results of this paper, the  $\chi^2$  distance will be used to find the similarity between descriptors of the two face images. It should be noted that the performance over PolyU-NIR is better than CASIA-NIR because only 20 samples per class are present in CASIA-NIR dataset, whereas PolyU-NIR dataset consists of more than 100 samples per subject.

Table 1. The values of the ARP for  $\eta = 10$ , ARR for  $\eta = 100$ , F\_score (F) and ANMRR using SVD-S-LBP descriptor over PolyU-NIR face database for different similarity measures. The best performance is observed with Chi-square distance measure.

Performance	Similarity Measures						
	Euclidean	Cosine	Emd	Canberra	L1	D1	$\chi^2$
ARP (%)	93.88	94.46	72.27	70.88	95.38	95.55	95.90
ARR (%)	44.08	45.41	29.32	31.50	47.07	47.41	48.85
F (%)	49.44	51.08	34.67	37.64	52.90	53.30	54.99
ANMRR (%)	45.59	43.91	62.84	60.31	41.97	41.56	39.82

Table 2. The values of the ARP for  $\eta = 10$ , ARR for  $\eta = 10$ , F\_score (F) and ANMRR using SVD-S-LBP descriptor over CASIA-NIR face database for different similarity measures. The best performance is observed with Chi-square distance measure.

Performance	Similarity Measures						
	Euclidean	Cosine	Emd	Canberra	L1	D1	$\chi^2$
ARP (%)	51.64	56.30	36.37	21.79	62.79	65.24	67.04
ARR (%)	25.82	28.15	18.18	10.90	31.40	32.62	33.52
F (%)	31.48	35.31	22.07	14.90	41.05	43.23	44.32
ANMRR (%)	63.93	59.98	74.48	83.18	54.13	51.92	50.72

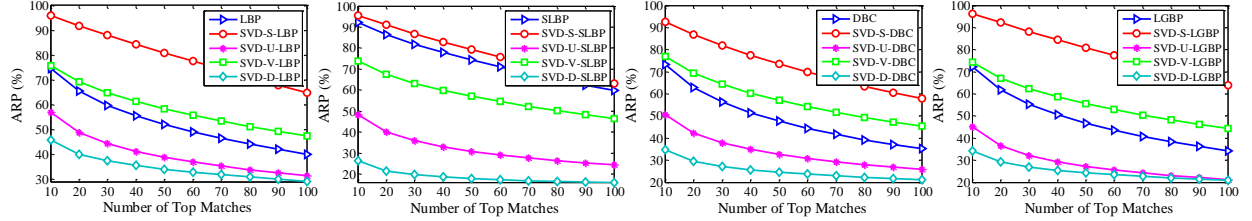


Fig. 5. The performance comparison of the local descriptors (i.e. LBP, SLBP, DBC and LGBP in the 1<sup>st</sup>, 2<sup>nd</sup>, 3<sup>rd</sup> and 4<sup>th</sup> column respectively) over different sub-bands of the SVD in terms of the ARP (%) vs  $\eta$  over PolyU-NIR face database. Clearly S sub-band is superior.

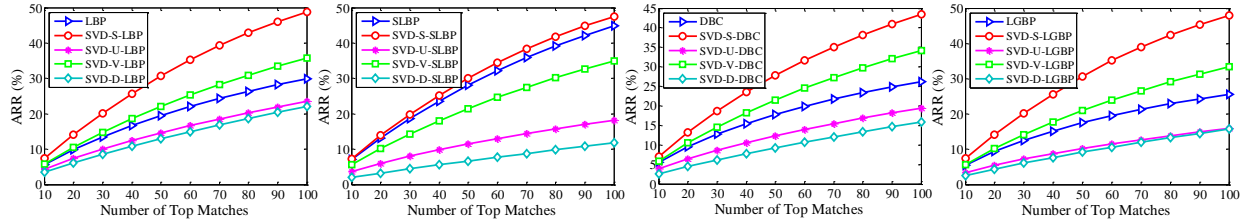


Fig. 6. The performance comparison of the local descriptors (i.e. LBP, SLBP, DBC and LGBP in the 1<sup>st</sup>, 2<sup>nd</sup>, 3<sup>rd</sup> and 4<sup>th</sup> column respectively) over different sub-bands of the SVD in terms of the ARR (%) vs  $\eta$  over PolyU-NIR face database. Clearly S sub-band is superior.

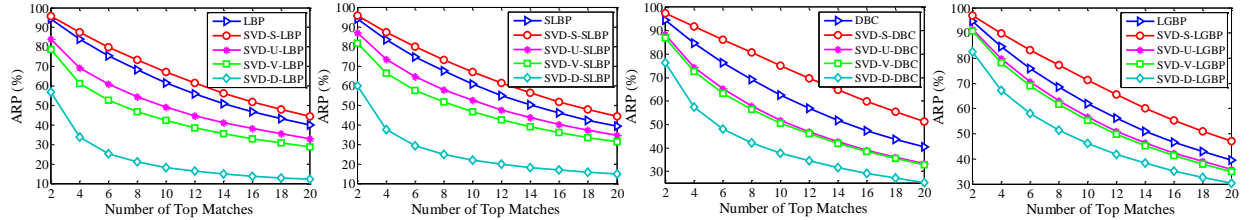


Fig. 7. The performance comparison of the local descriptors (i.e. LBP, SLBP, DBC and LGBP in the 1<sup>st</sup>, 2<sup>nd</sup>, 3<sup>rd</sup> and 4<sup>th</sup> column respectively) over different sub-bands of the SVD in terms of the ARP (%) vs  $\eta$  over CASIA-NIR face database. Clearly S sub-band outperforms others.

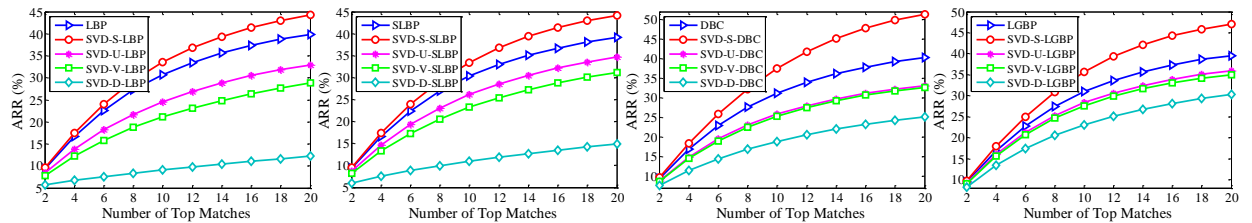


Fig. 8. The performance comparison of the local descriptors (i.e. LBP, SLBP, DBC and LGBP in the 1<sup>st</sup>, 2<sup>nd</sup>, 3<sup>rd</sup> and 4<sup>th</sup> column respectively) over different sub-bands of the SVD in terms of the ARR (%) vs  $\eta$  over CASIA-NIR face database. Clearly S sub-band outperforms others.

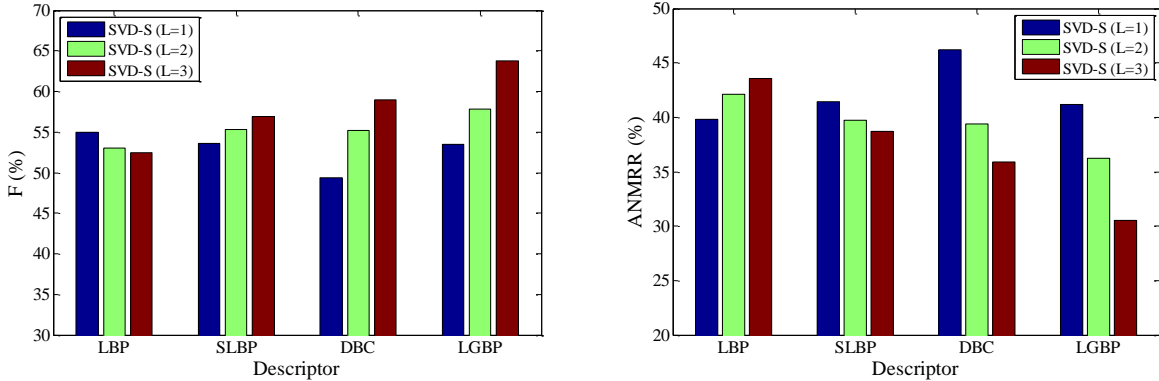
### B. Experiments over Different SVD Sub-bands

The local descriptors, including LBP, SLBP, DBC and LGBP over S, U, V and D sub-bands of SVD are compared using ARP vs  $\eta$  and ARR vs  $\eta$  over both PolyU-NIR and CASIA-NIR face databases in this experiment. In Fig. 5-8, the results over PolyU-NIR and CASIA-NIR databases are presented respectively. The performance of

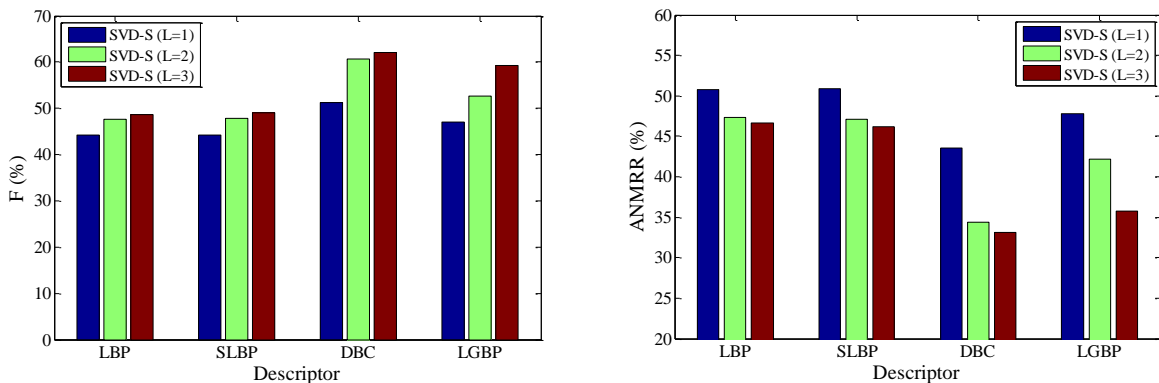
local descriptors degrades over U, V and D sub-bands in each case except for SVD-U-LBP, SVD-U-DBC and SVD-U-LGBP descriptor over PolyU-NIR database. A tremendous improvement in the performance is observed over S sub-band for each descriptor over each database. The {F-score, ANMRR} of SVD-S-LBP is improved by {63.22%, 36.85%} and {11.22%, 8.35%} as compared to the LBP over PolyU-NIR and CASIA-NIR database respectively. Note that in this paper, the improvement is presented in terms of the percentage improvement. The performance of SVD-S-DBC and SVD-S-LGBP is improved by {67.62%, 31.57%} and {86.99%, 39.76%} as compared to the DBC and LGBP respectively in terms of the {F-score, ANMRR} over PolyU-NIR database. The performance of SVD-S-LBP is also improved by 12.74% in terms of the F-score over CASIA-NIR database. The performance gain using SLBP is less because SLBP also incorporates the pre-processing step to enhance the local features. The results suggest that the S sub-band of SVD is more preferable than other sub-bands for computing the descriptors over it. The performance of local descriptors is only enhanced over the S sub-band because S sub-band have richer local information (by approximation), whereas, U, V and D sub-bands only contain the horizontal, vertical and diagonal information.

### C. Experiments over Level of SVD

We also investigated the effect of the level (L) of SVD factorization and compared the results for L=1, 2 and 3 using SVD-S-LBP, SVD-S-SLBP, SVD-S-DBC and SVD-S-LGBP descriptors in the Fig. 9(a-b) over the PolyU-NIR and CASIA-NIR face databases respectively in terms of the F (%) and ANMRR (%). It can be observed that the performance of each descriptor is improving (i.e. F-score is increasing and ANMRR is decreasing) at a higher level of SVD decomposition except for SVD-S-LBP over PolyU-NIR database. While we used the L=1 earlier in this paper, the performance can be increased further at a higher level of SVD decomposition. Thus, it is recommended to use SVD factorization at higher level.



(a) Over PolyU-NIR face database



(b) Over CASIA-NIR face database

Fig. 9. Comparison among different level of SVD decomposition using S sub-band in conjunction with different descriptors over (a) PolyU-NIR and (b) CASIA-NIR face databases in terms of the F (%) and ANMRR (%). The common trend can be observed that the performance improves at higher levels of S sub-band of SVD.

#### D. Retrieval Results

The top 10 matching retrieved faces are displayed for a query face from CASIA-NIR face database in Fig. 10 and for a query face image from PolyU-NIR face database in Fig. 11. The retrieval results are obtained using LBP, SVD-S-LBP, SLBP, SVD-S-SLBP, DBC, SVD-S-DBC, LGBP, and SVD-S-LGBP feature vectors in 1<sup>st</sup>, 2<sup>nd</sup>, 3<sup>rd</sup>, 4<sup>th</sup>, 5<sup>th</sup>, 6<sup>th</sup>, 7<sup>th</sup>, and 8<sup>th</sup> row respectively of Fig. 10-11. Note that the incorrect retrieved images are enclosed by a rectangle in Fig. 10(b) and Fig. 11(b). The precision over CASIA-NIR and PolyU-NIR face databases are {60%, 100%} and {70%, 100%} respectively, using {LBP, SVD-S-LBP} feature vectors as depicted in the 1<sup>st</sup> and 2<sup>nd</sup> row of Fig. 10-11. From 3<sup>rd</sup> and 4<sup>th</sup> row of Fig. 10, the number of correct matches are 8 and 10 using SLBP and SVD-S-LBP feature vectors respectively, over CASIA-NIR face database, whereas, it is 10 for both over PolyU-NIR face database as shown in the 3<sup>rd</sup> and 4<sup>th</sup> row of Fig. 11. The number of incorrect matches using DBC descriptor is 2 (see the 5<sup>th</sup> row of Fig. 10) and 3 (see the 5<sup>th</sup> row of Fig. 11) over CASIA-NIR and PolyU-NIR face databases respectively, whereas, it is 1 (see the 6<sup>th</sup> row of Fig. 10) and 0 (see the 6<sup>th</sup> row of Fig. 11) respectively, using SVD-S-DBC descriptor. The precision using LGBP and SVD-S-LGBP descriptors are 70% and 100% respectively over CASIA-NIR face database as displayed in the 7<sup>th</sup> and 8<sup>th</sup> row of the Fig. 10, while, it is 50% and 100% respectively over PolyU-NIR face database (see the 7<sup>th</sup> and 8<sup>th</sup> row of the Fig. 11).

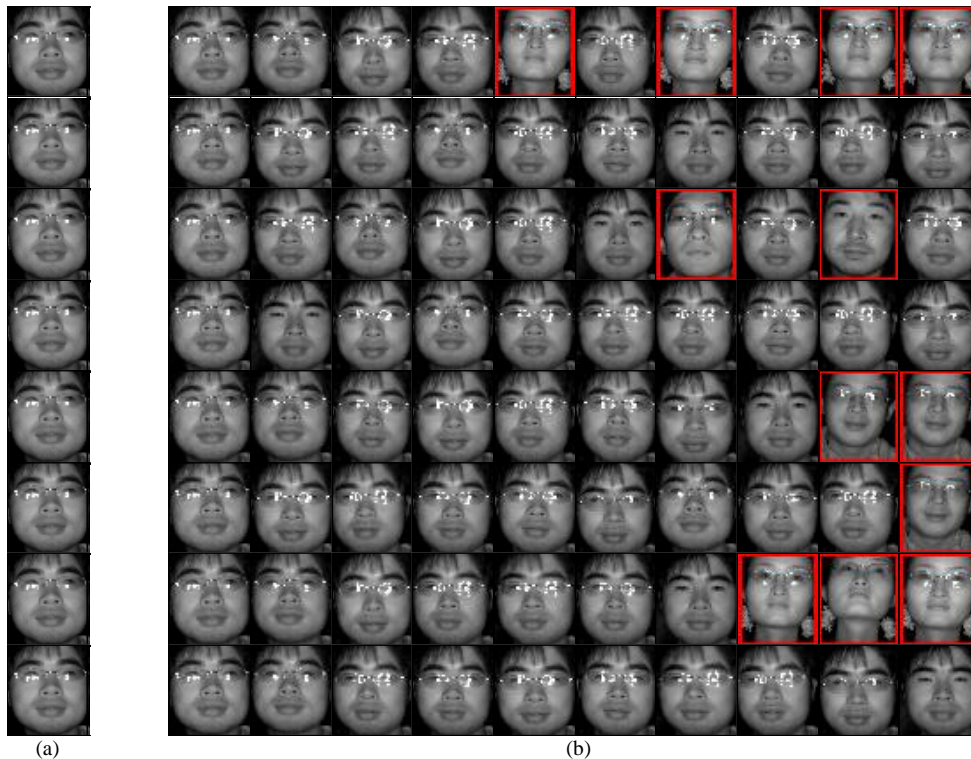


Fig. 10. Retrieval results from CASIA-NIR face database using LBP (1<sup>st</sup> row), SVD-S-LBP (2<sup>nd</sup> row), SLBP (3<sup>rd</sup> row), SVD-S-SLBP (4<sup>th</sup> row), DBC (5<sup>th</sup> row), SVD-S-DBC (6<sup>th</sup> row), LGBP (7<sup>th</sup> row) and SVD-S-LGBP (8<sup>th</sup> row) feature vectors, (a) query face, and (b) top 10 retrieved faces. The incorrect retrieved faces are enclosed in red color rectangles. It is noticed that the descriptors better perform with SVD S sub-band.

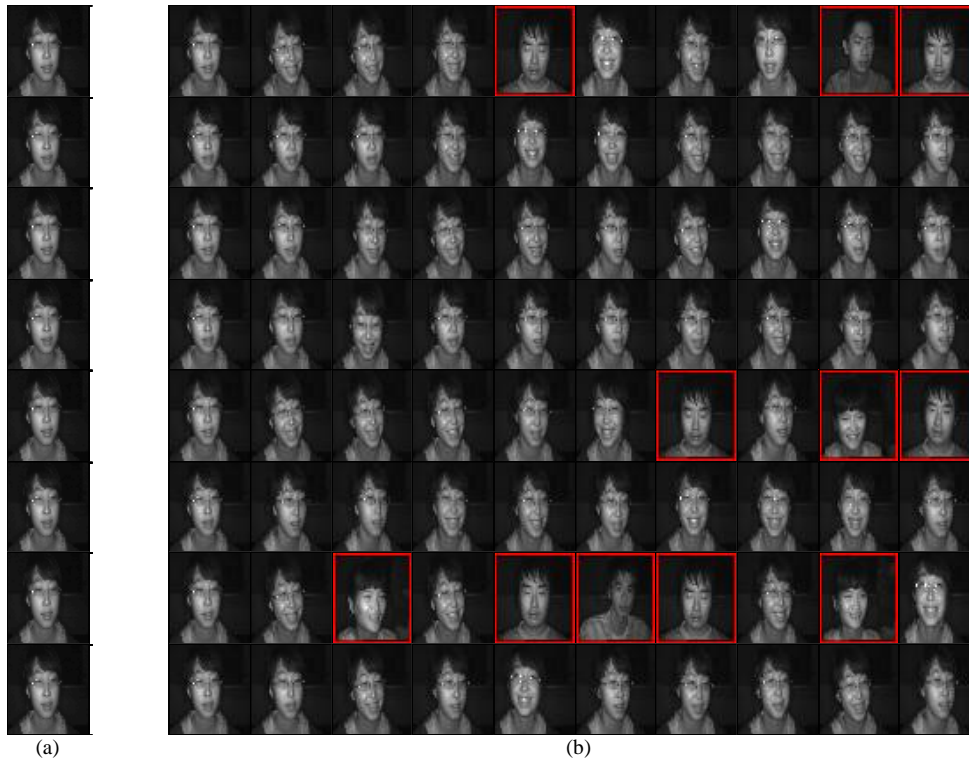
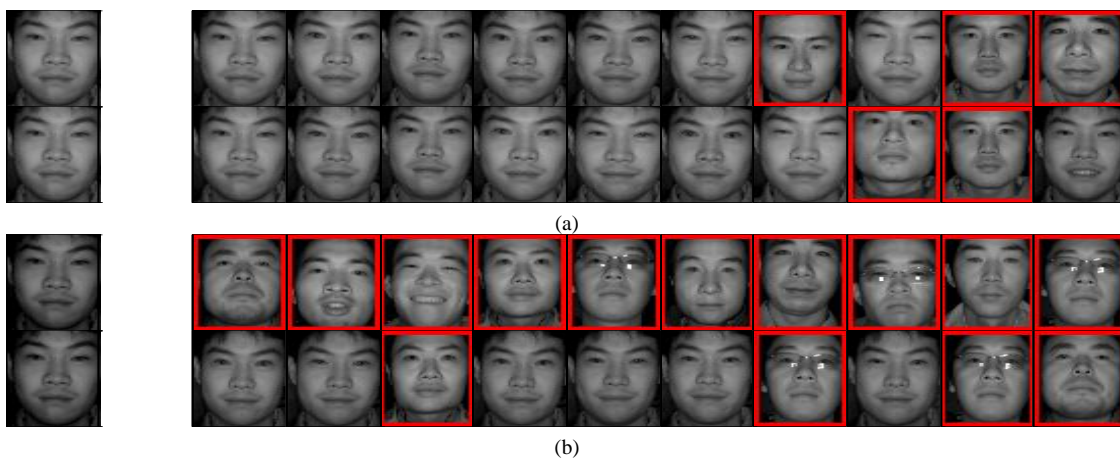


Fig. 11. Retrieval results from PolyU-NIR face database using LBP (1<sup>st</sup> row), SVD-S-LBP (2<sup>nd</sup> row), SLBP (3<sup>rd</sup> row), SVD-S-SLBP (4<sup>th</sup> row), DBC (5<sup>th</sup> row), SVD-S-DBC (6<sup>th</sup> row), LGBP (7<sup>th</sup> row) and SVD-S-LGBP (8<sup>th</sup> row) feature vectors, (a) query face, and (b) top 10 retrieved faces. Note that the faces in red color rectangles are the false positives. It is noticed that the descriptors better perform with SVD S sub-band.

In order to show the robustness of SVD-S sub-band against uniform intensity change, the top 10 retrieved images are displayed in Fig. 12 for different query images having uniform intensity differences. In the results of Fig. 12, 1<sup>st</sup> column shows the query images, the last 10 columns display the retrieved images, 1<sup>st</sup> row corresponds to the LBP without SVD, and 2<sup>nd</sup> row corresponds to the LBP with SVD. Fig. 12(a) basically considers a query face from CASIA-NIR face database. The query face in Fig. 12(b) is generated by subtracting 25 from the query face of Fig. 12(a). Similarly, the query face of Fig. 12(a) is added with 115 to generate the query face used in Fig. 12(c). From these results, it is observed that LBP alone fails completely in case of complex and uniform intensity change. Whereas, LBP with SVD still performs well. Thus, we can say that SVD increases the robustness against the complex illumination changes.



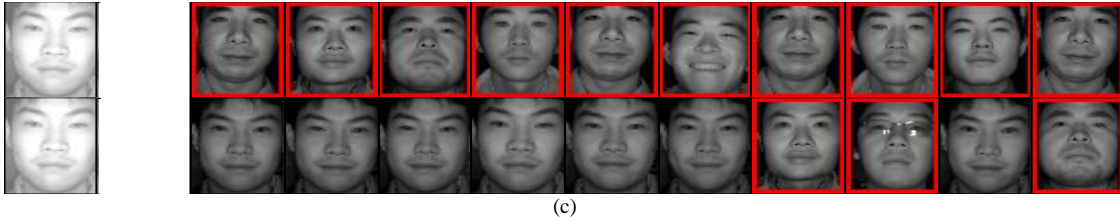


Fig. 12. Retrieval results to depict the robustness of SVD against uniform intensity change for (a) a query image from CASIA-NIR face database, (b) a query image generated by subtracting 25 from the query image of (a), and (c) a query image generated by adding 115 to the query image of (a). In each result 1<sup>st</sup> column is the query image, last 10 columns are the top 10 retrieved images, 1<sup>st</sup> row illustrates the results using LBP without SVD, and 2<sup>nd</sup> row illustrates the results using LBP with SVD. The incorrect retrieved faces are enclosed in red color rectangles.

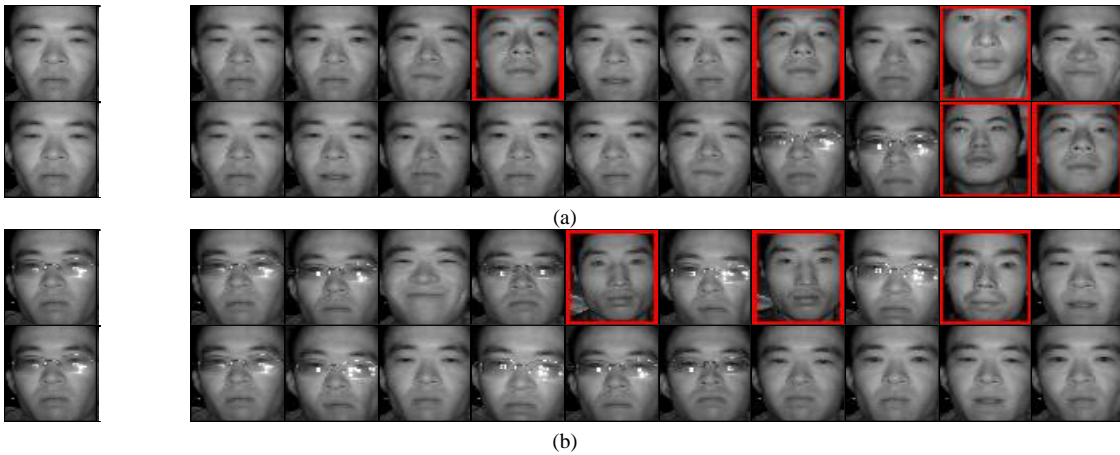


Fig. 13. Retrieval results to depict the robustness of SVD against the presence of spectacles. Top 10 matching faces for query images of a subject from CASIA-NIR face database, (a) without spectacles, and (b) with spectacles. In each result 1<sup>st</sup> column is the query image, last 10 columns are the top 10 retrieved images, 1<sup>st</sup> row illustrates the results using LBP without SVD, and 2<sup>nd</sup> row illustrates the results using LBP with SVD. The incorrect retrieved faces are enclosed in red color rectangles.

The retrieval results in Fig. 13 are dedicated to highlight the robustness of SVD towards occlusion basically presence of spectacles. In Fig. 13 also 1<sup>st</sup> column shows the query images, the last 10 columns display the retrieved images, 1<sup>st</sup> row corresponds to the LBP without SVD, and 2<sup>nd</sup> row corresponds to the LBP with SVD. Query images are considered from the same subject of CASIA-NIR face database. Fig. 13(a) uses query face without spectacles, whereas Fig. 13(b) considers with spectacles. The LBP alone is not able to retrieve even a single face with spectacles from the same subject in Fig. 13(a), whereas LBP with SVD does the better job. Similarly, in Fig. 13(b), LBP alone is not accurately matching the face having spectacle with a face without spectacles, whereas LBP with SVD retrieves more semantic faces from the same subject and achieves 100% precision for this example. This result clearly signifies the robustness of SVD against occlusion caused by spectacles.

Fig. 14 illustrates the retrieval results for two different expressions of a subject of CASIA-NIR face database. In each result of this experiment, 1<sup>st</sup> column is the query image, last 10 columns are the top 10 retrieved images, 1<sup>st</sup> row illustrates the results using LGBP without SVD, and 2<sup>nd</sup> row illustrates the results using LGBP with SVD. Note that, here we present the results using LGBP because LGBP is more discriminative than LBP. It is observed from these results that the LGBP with SVD achieves the 100% precision in both expressions and retrieves more semantically close images from the same subject. From Fig. 14, we can infer that SVD is better suited for different expressions in the database.



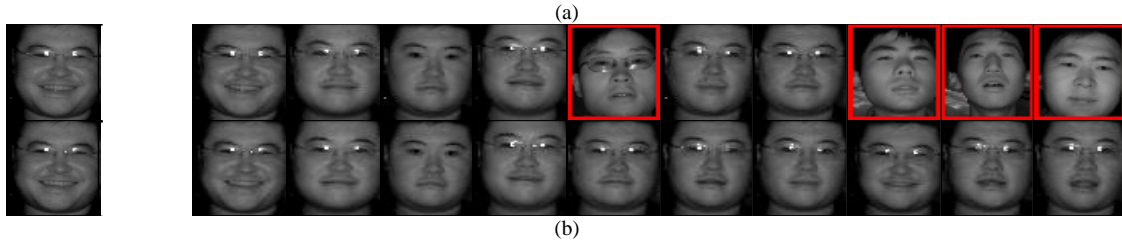


Fig. 14. Retrieval results to depict the robustness of SVD against expression. Top 10 matching faces for query images of a subject from CASIA-NIR face database, (a) normal expression, and (b) laugh expression. In each result 1<sup>st</sup> column is the query image, last 10 columns are the top 10 retrieved images, 1<sup>st</sup> row illustrates the results using LGBP without SVD, and 2<sup>nd</sup> row illustrates the results using LGBP with SVD. The incorrect retrieved faces are enclosed in red color rectangles.

From the experimental results, it is found that the proposed technique of computing the local descriptors over the S sub-band of SVD outperforms the local descriptors without SVD (i.e. the performance of local descriptor is boosted over S sub-band) under near-infrared face retrieval and confirms its discriminative ability as well as suitability. The SVD decomposition is able to cope with the low illumination problem of the near-infrared imaging in indoor and office environments.

#### E. Descriptor Dimension vs Time Analysis

In order to test the feature extraction and retrieval time complexity of the descriptors, we considered the 200 images from each PolyU-NIR and CASIA-NIR databases. The feature extraction of the database images is required to be done only once in content based image retrieval. Each time a query image is given as the input the feature extraction over only query image is required, whereas the for retrieval feature matching between the query image and each database image is required. We reported the total feature extraction time as well as total retrieval time for 200 images in Table 3 using the descriptors with and without SVD sub-band. It is observed that the feature extraction time of SVD based descriptors is quite high as compared to the original descriptors over both databases. This is due to the SVD factorization over  $2 \times 2$  non-overlapping sub-regions. Anyway, once feature extraction of whole databases is done prior to the image retrieval, only retrieval time is having the importance. As far as total retrieval time is concerned; it only depends upon the dimension of the descriptor for a fixed database. One of the most important characteristics of the SVD based descriptor is that its dimension is same as compared to the original descriptor.

Table 3. The total feature extraction time and total retrieval time in seconds over 200 images of each PolyU-NIR and CASIA-NIR database.

Metrics	Databases	Descriptors							
		LBP (256)	SVD-S-LBP (256)	SLBP (256)	SVD-S-SLBP (256)	DBC ( $8 \times 256$ )	SVD-S-DBC ( $8 \times 256$ )	LGBP ( $9 \times 256$ )	SVD-S-LGBP ( $9 \times 256$ )
Total Feature Extraction Time	PolyU-NIR	44	654	48	632	92	643	427	728
	CASIA-NIR	11	139	11	122	18	124	89	136
Total Retrieval Time	PolyU-NIR	0.24	0.26	0.22	0.24	2.27	2.25	2.55	2.57
	CASIA-NIR	0.24	0.22	0.22	0.21	1.25	1.2	1.39	1.31

In Table 3, it can be seen that the dimension of SVD-S-LBP (256) is same to LBP (256) which is 256, thus the total retrieval time for both the descriptors are also nearly same. Similarly, the total retrieval time using SVD-S-SLBP (256) is nearly same to SLBP (256) because its dimensions are same; the total retrieval time using SVD-S-DBC ( $8 \times 256$ ) is nearly same to DBC ( $8 \times 256$ ) as its dimensions are same; and the total retrieval time using SVD-S-LGBP ( $9 \times 256$ ) is same to LGBP ( $9 \times 256$ ) as its dimensions are same. So, from time analysis, it is revealed that the SVD sub-band based descriptors are not affecting the retrieval time as compared to the original descriptor without SVD sub-band.

## V. CONCLUSION

In this paper, we presented an image characterization approach for near-infrared face image retrieval by integrating the concepts of local SVD and local descriptors. Four sub-bands, namely S, U, V and D are created using local SVD factorization. The LBP, SLBP, DBC and LGBP feature descriptors are extracted over these SVD sub-

bands to form the various descriptors in conjunction with these sub-bands. The discriminating power and robustness of the proposed local descriptors is examined using the face retrieval experiments over two benchmark NIR face databases namely PolyU-NIR and CASIA-NIR. From the experiments, it is observed that the Chi-square distance is best suited for the similarity measurement. The performance of local descriptors over the S sub-band of the SVD is more preferable as compared to the other sub-bands. The discriminative ability of the local descriptors is further improved at a higher level of SVD decomposition of the previous S sub-band. Through experiments, it is confirmed that the performance of local descriptors boosted with SVD and outperforms the local descriptors without SVD over both NIR face databases. One of the limitations of the proposed method is the time complexity of the local SVD factorization over the blocks of the image.

#### REFERENCES

- [1] Y. Liu, D. Zhang, G. Lu, and W. Y. Ma, "A survey of content-based image retrieval with high-level semantics," *Pattern Recognition*, vol. 40, pp. 262–282, 2007.
- [2] A.W.M. Smeulders, M. Worring, S. Santini, A. Gupta, and R. Jain, "Content-based image retrieval at the end of the early years," *IEEE Trans. Pattern Anal. Mach. Intell.*, vol. 22, no. 12, pp. 1349–1380, Dec. 2000.
- [3] U. Park and A.K. Jain, "Face matching and retrieval using soft biometrics," *IEEE Transactions on Information Forensics and Security*, vol. 5, no. 3, pp. 406–415, 2010.
- [4] M. Hassaballah and S. Aly, "Face recognition: challenges, achievements and future directions," *IET Computer Vision*, vol. 9, no. 4, pp. 614–626, 2015.
- [5] A.K. Sao and B. Yegnanarayana, "Face verification using template matching," *IEEE Transactions on Information Forensics and Security*, vol. 2, no. 3, pp. 636–641, 2007.
- [6] Y. Pang, X. Li, Y. Yuan, D. Tao, and J. Pan, "Fast Haar transform based feature extraction for face representation and recognition," *IEEE Transactions on Information Forensics and Security*, vol. 4, no. 3, pp. 441–450, 2009.
- [7] Z. Chai, Z. Sun, H.M. Vazquez, R. He, and T. Tan, "Gabor ordinal measures for face recognition," *IEEE Transactions on Information Forensics and Security*, vol. 9, no. 1, pp. 14–26, 2014.
- [8] B. Zhang, L. Zhang, D. Zhang, and L. Shen, "Directional binary code with application to PolyU near-infrared face database," *Pattern Recognition Letters*, vol. 31, no. 14, pp. 2337–2344, 2010.
- [9] S.Z. Li, R.F. Chu, S.C. Liao, L. Zhang, "Illumination Invariant Face Recognition Using Near-infrared Images", *IEEE Transactions on Pattern Analysis and Machine Intelligence* (Special issue on Biometrics: Progress and Directions), vol.29, no.4, pp. 627–639, 2007.
- [10] K.P. Hollingsworth, S.S. Darnell, P.E. Miller, D.L. Woodard, K.W. Bowyer, and P.J. Flynn, "Human and machine performance on periocular biometrics under near-infrared light and visible light," *IEEE Transactions on Information Forensics and Security*, vol. 7, no. 2, pp. 588–601, 2012.
- [11] J.Y. Zhu, W.S. Zheng, J.H. Lai, and S.Z. Li, "Matching NIR Face to VIS Face Using Transduction," *IEEE Transactions on Information Forensics and Security*, vol. 9, no. 3, pp. 501–514, 2014.
- [12] S.R. Dubey, S.K. Singh, and R.K. Singh, "A multi-channel based illumination compensation mechanism for brightness invariant image retrieval", *Multimedia Tools and Applications*, vol. 74, no. 24, pp. 11223–11253, 2015.
- [13] S.R. Dubey, S.K. Singh, and R.K. Singh, "Rotation and scale invariant hybrid image descriptor and retrieval," *Computers & Electrical Engineering*, vol. 46, pp. 288–302, 2015.
- [14] S.R. Dubey, S.K. Singh, and R.K. Singh, "Local neighbourhood-based robust colour occurrence descriptor for colour image retrieval," *IET Image Processing*, vol. 9, no. 7, pp. 578–586, 2015.
- [15] T. Ojala, M. Pietikainen, and T. Maenpaa, "Multiresolution gray-scale and rotation invariant texture classification with local binary patterns", *IEEE Transactions on Pattern Analysis and Machine Intelligence*, vol. 24, no. 7, pp. 971–987, 2002.
- [16] Z. Guo and D. Zhang, "A completed modeling of local binary pattern operator for texture classification", *IEEE Transactions on Image Processing*, vol. 19, no. 6, pp. 1657–1663, 2010.
- [17] S.R. Dubey, S.K. Singh, and R.K. Singh, "Rotation and Illumination Invariant Interleaved Intensity Order Based Local Descriptor", *IEEE Transactions on Image Processing*, vol. 23, no. 12, pp. 5323–5333, 2014.
- [18] J. Ren, X. Jiang, J. Yuan, and G. Wang, "Optimizing LBP Structure For Visual Recognition Using Binary Quadratic Programming," *IEEE Signal Processing Letters*, vol. 21, no. 11, pp. 1346–1350, 2014.
- [19] S.R. Dubey, S.K. Singh, and R.K. Singh, "Local Diagonal Extrema Pattern: A new and Efficient Feature Descriptor for CT Image Retrieval", *IEEE Signal Processing Letters*, vol. 22, no. 9, pp. 1215–1219, 2015.
- [20] S.R. Dubey, S.K. Singh, and R.K. Singh, "Local Bit-plane Decoded Pattern: A Novel Feature Descriptor for Biomedical Image Retrieval," *IEEE Journal of Biomedical and Health Informatics*, vol. 20, no. 4, pp. 1139–1147, 2016.
- [21] G. Zhao, T. Ahonen, J. Matas, and M. Pietikainen, "Rotation-invariant image and video description with local binary pattern features", *IEEE Transactions on Image Processing*, vol. 21, no. 4, pp. 1465–1477, 2012.
- [22] D. Huang, C. Shan, M. Ardabilian, Y. Wang, and L. Chen, "Local binary patterns and its application to facial image analysis: a survey", *IEEE Transactions on Systems, Man, and Cybernetics, Part C: Applications and Reviews*, vol. 41, no. 6, pp. 765–781, 2011.
- [23] T. Ahonen, A. Hadid, and M. Pietikainen, "Face description with local binary patterns: Application to face recognition", *IEEE Transactions on Pattern Analysis and Machine Intelligence*, vol. 28, no. 12, pp. 2037–2041, 2006.
- [24] K. Jeong, J. Choi, and G. Jang, "Semi-Local Structure Patterns for Robust Face Detection", *IEEE Signal Processing Letters*, vol. 22, no. 2, pp. 1400–1403, 2015.
- [25] W. Zhang, S. Shan, W. Gao, X. Chen, and H. Zhang, "Local gabor binary pattern histogram sequence (lgbphs): A novel non-statistical model for face representation and recognition," In *Tenth IEEE International Conference on Computer Vision*, pp. 786–791, 2005.
- [26] B. Zhang, Y. Gao, S. Zhao, and J. Liu, "Local derivative pattern versus local binary pattern: face recognition with high-order local pattern descriptor", *IEEE Transactions on Image Processing*, vol. 19, no. 2, pp. 533–544, 2010.
- [27] D. Huang, M. Ardabilian, Y. Wang, and L. Chen, "3-d face recognition using elbp-based facial description and local feature hybrid matching," *IEEE Transactions on Information Forensics and Security*, vol. 7, no. 5, pp. 1551–1565, 2012.

- [28] H.T. Nguyen and A. Caplier, "Local Patterns of Gradients for Face Recognition," *IEEE Transactions on Information Forensics and Security*, vol.10, no. 8, pp. 1739-1751, 2015.
- [29] N.S. Vu, "Exploring patterns of gradient orientations and magnitudes for face recognition," *IEEE Transactions on Information Forensics and Security*, vol. 8, no. 2, pp. 295-304, 2013.
- [30] M. Yang, L. Zhang, S.K. Shiu, and D. Zhang, "Monogenic binary coding: An efficient local feature extraction approach to face recognition," *IEEE Transactions on Information Forensics and Security*, vol. 7, no. 6, pp. 1738-1751, 2012.
- [31] T. Konda and Y. Nakamura, "A new algorithm for singular value decomposition and its parallelization", *Parallel Computing*, vol. 35, no. 6, pp. 331-344, 2009.
- [32] H. Andrews and C. Patterson, "Singular value decompositions and digital image processing", *IEEE Transactions on Acoustics, Speech and Signal Processing*, vol. 24, no. 1, pp. 26-53, 1976.
- [33] K. Konstantinides, B. Natarajan, and G.S. Yovanof, "Noise estimation and filtering using block-based singular value decomposition", *IEEE Transactions on Image Processing*, vol. 6, no. 3, pp. 479-483, 1996.
- [34] R. Kakarala and P.O. Ogunbona, "Signal analysis using a multiresolution form of the singular value decomposition", *IEEE Transactions on Image Processing*, vol. 10, no. 5, pp. 724-735, 2001.
- [35] S. Wei, A. Nahapetian, M. Nelson, F. Koushanfar, and M. Potkonjak, "Gate characterization using singular value decomposition: Foundations and applications," *IEEE Transactions on Information Forensics and Security*, vol. 7, no. 2, pp. 765-773, 2012.
- [36] J.F. Yang and C.L. Lu, "Combined techniques of singular value decomposition and vector quantization for image coding", *IEEE Transactions on Image Processing*, vol. 4, no. 8, pp. 1141-1146, 1995.
- [37] R. Liu and T. Tan, "An SVD-based watermarking scheme for protecting rightful ownership", *IEEE Transactions on Multimedia*, vol. 4, no. 1, pp. 121-128, 2002.
- [38] G. Gul and F. Kurugollu, "SVD-based universal spatial domain image steganalysis," *IEEE Transactions on Information Forensics and Security*, vol. 5, no. 2, pp. 349-353, 2010.
- [39] S.K. Singh and S. Kumar, "A Framework to Design Novel SVD Based Color Image Compression", *In the Proceedings of the Third UKSim European Symposium on Computer Modeling and Simulation*, pp. 235-240, 2009.
- [40] G. Bhatnagar, A. Saha, Q.M.J. Wu, and P.K. Atrey, "Analysis and extension of multiresolution singular value decomposition", *Information Sciences*, vol. 277, pp. 247-262, 2014.
- [41] S.K. Singh and S. Kumar, "Singular value decomposition based sub-band decomposition and multi-resolution (SVD-SBD-MRR) representation of digital colour images", *Pertanika Journal of Science and Technology*, vol. 19, no. 2, pp. 229-235, 2011.
- [42] W. Kim, S. Suh, W. Hwang, and J-J. Han, "SVD Face: Illumination-Invariant Face Representation," *IEEE Signal Processing Letters*, vol. 21, no. 11, pp. 1336-1340, 2014.
- [43] K.P. Chandar, M.M. Chandra, M.R. Kumar, and B. Swarnalatha, "Preprocessing using SVD towards illumination invariant face recognition," *In Proc. of Recent Advances in Intelligent Computational Systems*, pp. 051-056, 2011.
- [44] "PolyU-NIR Face Database, [http://www.comp.polyu.edu.hk/~biometrics/NIRFace/polyudb\\_face.htm](http://www.comp.polyu.edu.hk/~biometrics/NIRFace/polyudb_face.htm)".
- [45] "CASIA-NIR Face Database, [http://www.cbsr.ia.ac.cn/english/NIR\\_face%20Databases.asp](http://www.cbsr.ia.ac.cn/english/NIR_face%20Databases.asp)".
- [46] [www.cs.columbia.edu/~mmerler/project/code/pdist2.m](http://www.cs.columbia.edu/~mmerler/project/code/pdist2.m).
- [47] S. Murala and Q.M.J. Wu, "Local ternary co-occurrence patterns: A new feature descriptor for MRI and CT image retrieval," *Neurocomputing*, vol. 119, pp. 399-412, 2013.
- [48] K. Lu, N. He, J. Xue, J. Dong, and L. Shao, "Learning View-Model Joint Relevance for 3D Object Retrieval", *IEEE Transactions on Image Processing*, vol. 24, no. 5, pp. 1449-1459, 2015.
- [49] <http://www.cse.oulu.fi/CMV/Downloads/LBPMatlab>.
- [50] S.R. Dubey, S.K. Singh, and R.K. Singh, "Local wavelet pattern: A new feature descriptor for image retrieval in medical CT databases", *IEEE Transactions on Image Processing*, vol. 24, no. 12, pp. 5892-5903, 2015.
- [51] S.R. Dubey, S.K. Singh, and R.K. Singh, "Multichannel Decoded Local Binary Patterns for Content-Based Image Retrieval", *IEEE Transactions on Image Processing*, vol. 25, no. 9, pp. 4018-4032, 2016.
- [52] L. Li, J. Gao, and H. Ge, "A new face recognition method via semi-discrete decomposition for one sample problem", *Optik-International Journal for Light and Electron Optics*, vol. 127, no. 19, pp. 7408-7417, 2016.
- [53] L. Li, H. Ge, and J. Gao, "Maximum-minimum-median average MSD-based approach for face recognition", *AEU-International Journal of Electronics and Communications*, vol. 70, no. 7, pp. 920-927, 2016.
- [54] J. Gao, L. Fan, and L. Xu, "Median null (sw)-based method for face feature recognition", *Applied Mathematics and Computation*, vol. 219, no. 12, pp. 6410-6419, 2013.
- [55] J. Gao, L. Fan, and L. Xu, "Solving the face recognition problem using QR factorization", *WSEAS Transactions on Mathematics*, vol. 11, no. 8, pp. 728-737, 2012.
- [56] J. Gao and L. Fan, "Kernel-based weighted discriminant analysis with QR decomposition and its application face recognition", *WSEAS Transactions on Mathematics*, vol. 10, no. 10, pp. 358-367, 2011.
- [57] J. Gao, L.Y. Fan, L. Li, and L.Z. Xu, "A practical application of kernel-based fuzzy discriminant analysis", *International Journal of Applied Mathematics and Computer Science*, vol. 23, no. 4, pp. 887-903, 2013.